# Enhanced thermal stability and nanoparticle-mediated surface patterning: $Pt/TiO_2(110)$

A. Naitabdi,[1] F. Behafarid,[1] and B. Roldan Cuenya[1,2,a)]
[1]*Department of Physics, University of Central Florida, Orlando, Florida 32816, USA*
[2]*Nanoscience and Technology Center, University of Central Florida, Orlando, Florida 32816, USA*

(Received 8 December 2008; accepted 27 January 2009; published online 23 February 2009)

This letter reports (i) the enhanced thermal stability (up to 1060 °C) against coarsening and/or desorption of self-assembled Pt nanoparticles synthesized by inverse micelle encapsulation and deposited on $TiO_2(110)$ and (ii) the possibility of taking advantage of the strong nanoparticle/support interactions present in this system to create patterned surfaces at the nanoscale. Following our approach, $TiO_2$ nanostripes with tunable width, orientation, and uniform arrangement over large surface areas were produced. © *2009 American Institute of Physics*. [DOI: 10.1063/1.3083557]

Strong metal-support interactions[1,2] are believed to be a key factor determining the reactivity of heterogeneous catalysts such as Pt nanoparticles (NPs) supported on $TiO_2$. Most of the past research efforts in this field considered vacuum evaporated, chemical vapor deposited, or electron-beam synthesized Pt NPs as model systems. Two common trends were identified: the onset of NP coalescence upon annealing below ~430 °C (Ref. 3) and NP encapsulation by $TiO_x$ compounds.[1,2] Both effects were found to dramatically affect the electronic[1] and catalytic[3] properties of this system.

It is well known that the NP size is one of the crucial parameters determining the activity and selectivity of supported nanocatalysts.[4–6] At elevated operation temperatures, the performance of industrial catalysts is strongly influenced by NP coarsening, commonly leading to catalyst deactivation. In order to minimize these undesirable effects, stable arrays of NP catalysts homogenously dispersed on a support are needed.[7–9] Additionally, the structure, chemical composition, and stability of the NP support are also essential in maintaining the reactivity of supported clusters. Interestingly, the presence of the NPs can affect the stability of the support. For example, the dissolution of Pt during $O_2$ reduction in an electrochemical environment was found to be reduced in the presence of Au NPs.[10] Therefore, the design of a stable support-metal NP system requires a thorough understanding of the changes in the electronic, chemical, and morphological properties of the support induced by the NPs.

In this letter we will show that particle size selection and enhanced thermal stability (up to 1060 °C) can be achieved when Pt NPs (~3 nm in height) are synthesized by micelle encapsulation and deposited on $TiO_2(110)$. Furthermore, the ordered NP array achieved can be utilized to pattern the underlying substrate into $TiO_2$ nanostripes with tunable width, orientation, and separation. This opens the possibility of tailoring the morphological structure of a catalytic support at the nanoscale level.

Self-assembled size-selected Pt NPs were synthesized by encapsulation in diblock-copolymer micelles formed by dissolving polystyrene-block-poly(2-vinylpyridine) [PS($x$)-P2VP($y$)] (with molecular weights $x=27\,700$ and $y=4300$ g/mol) in toluene. Subsequently, $H_2PtCl_6 \cdot 6H_2O$ was added to the polymeric solution at a metal salt to PS-P2VP concentration ratio of 0.6. The NP size is controlled by the length of the polymer head (P2VP) and the metal-salt/P2VP concentration ratio, while the interparticle distance is determined by the length of the polymer tail (PS). A monolayer-thick film of NPs was obtained by dip coating (*ex situ*) a $TiO_2(110)$ single crystal into the Pt polymeric solution. The $TiO_2$ substrate was previously cleaned in ultrahigh vacuum (UHV) by $Ar^+$ sputtering (1 keV) and annealing cycles at 950 °C and then exposed to air. The sample was then introduced into a UHV system (SPECS, GmbH) for chemical and morphological characterizations. The encapsulating polymer was removed *in situ* by $O_2$-plasma exposure ($4 \times 10^{-5}$ mbar, 95 min). Complete removal of the organic ligands was evidenced by the lack of C 1*s* signal in x-ray photoelectron spectroscopy (XPS) measurements. Subsequently, the sample was isochronally annealed *in situ* in 100 °C intervals (20 min) from 300 to 900 °C, and in 10 °C intervals (10 min) from 1000 to 1060 °C. XPS (not shown) and scanning tunneling microscopy (STM) (Aarhus-SPECS) data were acquired after several thermal treatments (Figs. 1 and 2).

Figure 1 displays STM images of Pt NPs deposited on $TiO_2(110)$ after polymer removal by atomic oxygen exposure and annealing at (a) 300 and (b) 1000 °C. Surprisingly, neither the NP size nor their surface distribution was found to change significantly upon annealing at 1000 °C [Fig. 1(b)]. However, a decrease in the roughness of the $TiO_2$ support (induced by the initial $O_2$-plasma treatment) from

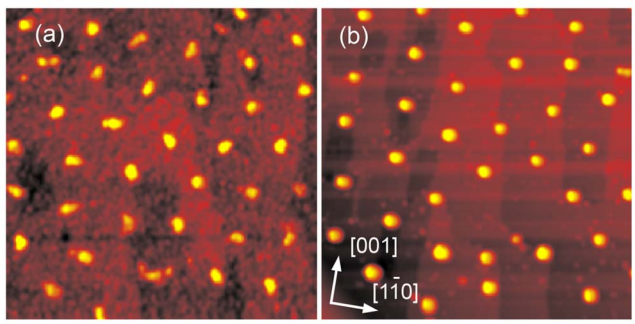


FIG. 1. (Color online) ($200 \times 200$ nm$^2$) *In situ* STM images of Pt NPs deposited on $TiO_2(110)$ after an $O_2$-plasma treatment and annealing in UHV at (a) 300 °C for 20 min and (b) 1000 °C for 10 min.

a)Electronic mail: roldan@physics.ucf.edu.

 

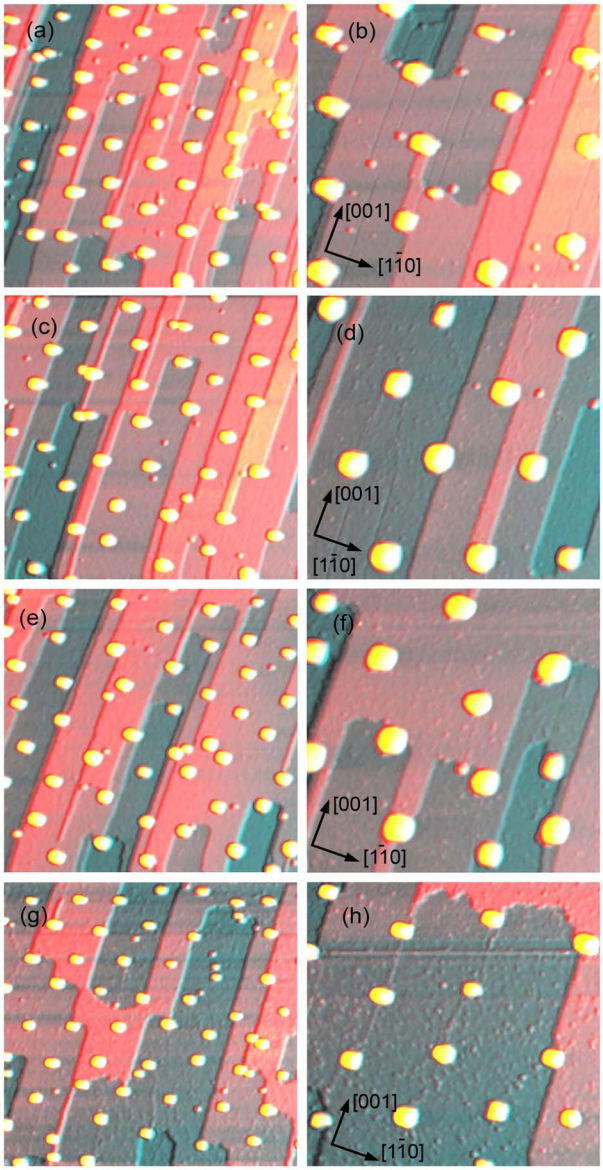


FIG. 2. (Color online) *In situ* STM images of Pt NPs deposited on $TiO_2$(110) acquired after $O_2$-plasma and subsequent annealing for 10 min in UHV at [(a) and (b)] 1010 °C, [(c) and (d)] 1040 °C, [(e) and (f)] 1060 °C, and [(g) and (h)] second 1060 °C. The size of the images in the left column is $200\times200$ nm$^2$ and in the right column is $100\times100$ nm$^2$.

$0.3\pm0.05$ nm after subsequent annealing at 300 °C to $0.07\pm0.03$ nm at 1000 °C with a $(1\times2)$ surface reconstruction can be seen. Further stepwise annealing from 1010 to 1060 °C [Figs. 2(a)–2(f)] demonstrated the enhanced thermal stability and low mobility of our Pt NPs. Only upon annealing at 1060 °C for an additional 10 min [Figs. 2(g) and 2(h)] were small changes in the NP size and in the local NP arrangement noticed.

Figure 3 shows histograms of the (a) NP height and (b) interparticle distance obtained from the analysis of numerous STM images acquired after different *in situ* thermal treatments from 1000 to 1060 °C. The data in Fig. 3(a) indicate that the average NP height is nearly constant up to the first annealing treatment at 1060 °C for 10 min ($3.4\pm0.2$ nm). However, a clear increase in the width of the NP height distribution and bimodal shape is observed upon further annealing at the same temperature (1060 °C, 20 min), with average peak heights in the distribution of 3.2 and 2.3 nm. In addition, the width of the height distribution increased from 0.9 nm at 1000 °C to 1.6 nm at 1060 °C (second). These effects are attributed to atomic Pt desorption rather than to Ostwald ripening, since no increase in the average number of large NPs was observed.

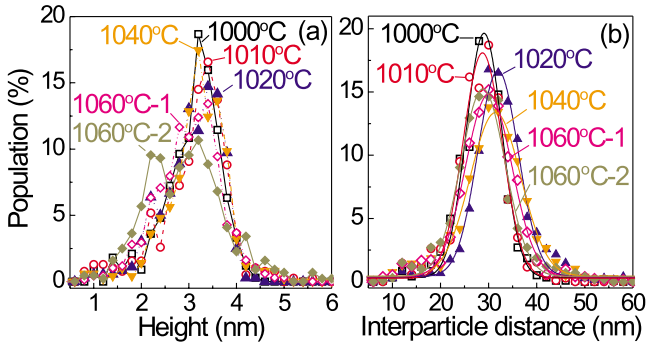


FIG. 3. (Color online) Normalized histograms of (a) NP height and (b) interparticle distance obtained from STM images acquired after isochronal annealing in 10 °C intervals (10 min) from 1010 to 1060 °C. The lines in (a) are guides for the eyes, while the data in (b) were fitted using Gaussian curves. For each temperature, the above statistics include 300–670 NPs.

The nearest-neighbor interparticle distance histograms shown in Fig. 3(b) demonstrate that our initial hexagonal NP arrangement is basically preserved after high temperature annealing, with an average interparticle distance (peak of the distribution) of $30\pm2$ nm from 1000 to 1060 °C. If entire NPs were to desorb at high temperature, a shift in the histogram peak toward higher interparticle distances should have been observed. Significant particle mobility would have led to a broadening of the interparticle distance distribution and a corresponding reduction in the peak height. A small increase in the width (standard deviation) of the interparticle distance distribution (from ~7.3 nm at 1000 °C to 9.1 nm at 1060 °C, 20 min anneal) and a decrease in its height (peak population) can be observed above 1040 °C. This result might indicate a weakening of the NP-support adhesion and the consequent onset of NP mobility. Since after our second annealing at 1060 °C some smaller particles (~2.3 nm) are present on the sample, the possibility of particle break up and local cluster mobility is more likely. Despite the observation of some local disorder, the majority of our scans still showed clear signs of a hexagonal NP arrangement up to at least the first thermal treatment at 1060 °C.

A striking observation is the formation of $TiO_2$ nanostripes running preferentially along the [001] direction in the Pt-decorated samples upon annealing above 1000 °C [Figs. 2 and 4(a)]. Such narrow terraces or nanostripes are not observed when the NP-free substrate is subjected to the same thermal treatment [Fig. 4(b)]. Interestingly, the width of these nanostripes seems to be related to the size of the NPs and their spatial distribution to the interparticle distance. The average width of the $TiO_2$ terraces on the Pt-decorated samples was ~16 nm at 1010 °C, ~23 nm at 1060 °C (10 min), and increased to ~47 nm at 1060 °C (20 min). For comparison, at 1030 °C, a larger average terrace width of ~80 nm was measured for the Pt-free $TiO_2$(110) support. In addition, the ratio of the length of [001] to [1$\bar{1}$1] steps was much higher for the Pt-decorated surface (~11) as compared to pristine $TiO_2$ (~2.4). From the analysis of multiple $200\times200$ nm$^2$ STM images of our Pt/$TiO_2$ system, a strong decrease in the total length of the steps parallel to [001] was

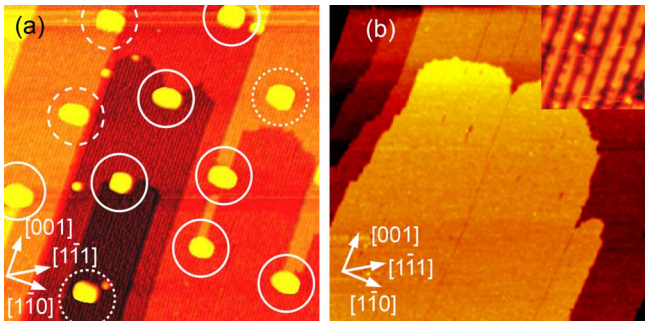


FIG. 4. (Color online) ($100\times100$ nm$^2$) STM images obtained on (a) Pt NPs deposited on $TiO_2$(110) and (b) the pristine $TiO_2$(110) substrate after annealing at 1060 and 1030 °C for 10 min, respectively. Insert in (b): ($7\times7$ nm$^2$) region of the atomically resolved $TiO_2$ surface. The circles in (a) indicate the presence of NPs at different sites: (1) on the center of $TiO_2$ terraces (dotted), (2) on steps parallel to the [001] direction (dashed), (3) NPs at the end of $TiO_2$ nanostripes, or at [1$\bar{1}$1] steps (full).

observed with increasing annealing temperature. Measured lengths ranged from ~2430 nm at 1010 °C to ~1730 and ~853 nm for the 10 and 20 min annealing treatments at 1060 °C, respectively. A similar analysis revealed significantly shorter lengths for the steps parallel to [1$\bar{1}$1], with ~227 nm at 1010 °C, ~130 nm at 1060 °C (10 min), and ~236 nm at 1060 °C (20 min).

Surprisingly, the $TiO_2$ stripes and steps were found to be rather straight, and a large population of the $TiO_2$ stripes was found to have one NP at the end. Statistics of the location of the Pt NPs in our samples after annealing (averaging 340–690 NPs at each temperature) revealed that 45% of the NPs are located at the end of stripes at steps parallel to [1$\bar{1}$1] at 1000 °C [white circles in Fig. 4(a)], while at 1060 °C (20 min) they tend to be located on the middle of terraces (40% versus 25% at this location at 1000 °C). Since the initial NP arrangement was preserved, this result is not attributed to the migration of Pt NPs to those step sites, but to the mobility of Ti–O molecules or Ti and O atoms in the support. Berko *et al.*[11] reported that Pt atoms activate the separation of $Ti_xO_y$ compounds and a preferential atomic diffusion along [001] was described. Besides, our data reveal that the bonding between the Pt atoms and the $TiO_2$ substrate is strongest at step sites.[11] Sample annealing at our highest temperature (1060 °C, 20 min) resulted in a rupture of the connection between many of our NPs and the $TiO_2$ nanostripes, leading to the increase in the $TiO_2$ terrace width.

The observations made here are markedly different from existing studies on UHV-grown NPs deposited on $TiO_2$ surfaces,[12–16] which showed preferential step decoration and NP coarsening at relatively low temperatures. The high stability of our micellar Pt/$TiO_2$(110) system may be the result of our unique synthesis procedure, structure, and morphology. For example, the initial $O_2$-plasma treatment to which our NPs were exposed results in the presence of O-adatoms on the $TiO_2$(110) surface, and stronger bonding of metal NPs to such a surface has been previously reported.[17] Alternatively, small amounts of carbon (not detectable by XPS) might be present underneath the NPs or at the NP/support perimeter in the form of TiC compounds that could contribute to the stabilization of the NPs. Furthermore, in contrast with UHV evaporated NP samples, our size-selected three-dimensional-like spherical NP samples have relatively large interparticle distances and Pt atoms or small Pt seeds are not present between larger NPs, making Ostwald ripening processes less favorable.

In summary, we demonstrated high thermal stability and enhanced particle-support adhesion of Pt NPs prepared by micelle encapsulation on $TiO_2$. No mobility (as a whole or through Ostwald ripening) is observed up to at least 1060 °C. Significant substrate surface restructuring is observed at annealing temperatures above 1000 °C, leading to the formation of $TiO_2$ nanostripes with a width that appears to be affected by the NP size. This type of micelle-generated particle array may lead to high-temperature nanocatalysts with tunable substrate structure.

This work was supported by the U.S. Department of Energy (Grant No. DE-FG02-08ER15995).

[1] O. Dulub, W. Hebenstreit, and U. Diebold, Phys. Rev. Lett. **84**, 3646 (2000).
[2] F. Pesty, H. P. Steinruck, and T. E. Madey, Surf. Sci. **339**, 83 (1995).
[3] D. N. Belton, Y. M. Sun, and J. M. White, J. Phys. Chem. **88**, 1690 (1984).
[4] T. Akita, K. Tanaka, S. Tsubota, and M. Haruta, J. Electron Microsc. **49**, 657 (2000).
[5] L. K. Ono, D. Sudfeld, and B. Roldan Cuenya, Surf. Sci. **600**, 5041 (2006).
[6] J. R. Croy, S. Mostafa, J. Liu, Y. H. Sohn, and B. Roldan Cuenya, Catal. Lett. **118**, 1 (2007).
[7] C. R. Henry, Surf. Sci. Rep. **31**, 231 (1998).
[8] A. S. Eppler, G. Rupprechter, E. A. Anderson, and G. A. Somorjai, J. Phys. Chem. B **104**, 7286 (2000).
[9] K. H. Hansen, T. Worren, S. Stempel, E. Laegsgaard, M. Baumer, H. J. Freund, F. Besenbacher, and I. Stensgaard, Phys. Rev. Lett. **83**, 4120 (1999).
[10] J. Zhang, K. Sasaki, E. Sutter, and R. R. Adzic, Science **315**, 220 (2007).
[11] A. Berko, O. Hakkel, J. Szoko, and F. Solymosi, Surf. Sci. **507**, 643 (2002).
[12] S. C. Parker and C. T. Campbell, Phys. Rev. B **75**, 035430 (2007).
[13] A. El-Azab, S. Gan, and Y. Liang, Surf. Sci. **506**, 93 (2002).
[14] M. J. J. Jak, C. Konstapel, A. van Kreuningen, J. Verhoeven, and J. W. M. Frenken, Surf. Sci. **457**, 295 (2000).
[15] P. Stone, S. Poulston, R. A. Bennett, and M. Bowker, Chem. Commun. (Cambridge) **1998**, 1369.
[16] X. Lai, T. P. St Clair, M. Valden, and D. W. Goodman, Prog. Surf. Sci. **59**, 25 (1998).
[17] D. Matthey, J. G. Wang, S. Wendt, J. Matthiesen, R. Schaub, E. Laegsgaard, B. Hammer, and F. Besenbacher, Science **315**, 1692 (2007).